ELSEVIER

Journal of Alloys and Compounds 452 (2008) 291–297

Journal of ALLOYS AND COMPOUNDS

www.elsevier.com/locate/jallcom

IMC formation on BGA package with Sn–Ag–Cu and Sn–Ag–Cu–Ni–Ge solder balls

Kwang-Lung Lin, Po-Cheng Shih *

Department of Materials Science and Engineering, National Cheng-Kung University, No. 1, Ta-Hsueh Road, Tainan 701, Taiwan, ROC

Received 10 August 2006; received in revised form 6 November 2006; accepted 6 November 2006
Available online 6 February 2007

Abstract

Solder balls were attached to the Cu/Ni–P/Au metallized BGA substrate. The two solder ball used in this study are Sn–3.2Ag–0.5Cu and Sn–3.5Ag–0.5Cu–0.07Ni–0.01Ge. The package was subjected to thermal aging at 150 °C for 100–1000 h in order to investigate IMC formation behavior. Cross sections and the surface of the IMC layer, revealed through etching of the unreacted solder, were inspected and analyzed with SEM and EDX. The IMCs mainly consist of two morphologies, hexagonal and whisker. The hexagonal crystal was identified as $(Cu, Ni)_6Sn_5$ and the whisker crystal is $(Ni, Cu)_3Sn_4$. The dissolution of Ni in Cu_6Sn_5 results in a synergistic effect that enhances the growth of the compound, and a similar effect was not observed when dissolved Cu was present in Ni_3Sn_4. This phenomenon is possibly due to the vacant energy band of the 3d-orbital of Ni. Ag_3Sn was also detected in the solder region near the interfacial IMC. The Ag_3Sn was not in direct contact with the BGA substrate.

Keyword: Intermetallics

1. Introduction

Among the various solder alloy systems, Sn–Ag–Cu lead-free solder has been suggested as one of the promising candidates to replace the Pb-bearing solders used in electronics packaging [1–5]. The ternary eutectic reaction of Sn–Ag–Cu solder takes place in the composition range of 3.2–4.7 wt.% Ag and 0.5–1.7 wt.% Cu at 217 °C [2]. Moreover, this solder provides good solderability and good mechanical properties [3,4]. However, the ternary eutectic point (217 °C) of Sn–Ag–Cu is much higher than that of the Sn-Pb eutectic point (183 °C), and this is expected to result in the excessive growth of intermetallic compounds (IMCs) during the soldering process [5]. The overgrown IMCs are detrimental to the bonding strength between solder and substrate due to increased brittleness. In general, in order to control the interfacial reactions, the Ni-P electroless layer was often used as diffusion barrier to inhibit Cu dissolution and IMC formation, and an immersion Au layer is plated on Ni-P layer to prevent surface oxidation. Previous studies [6–8] indicated that two types of ternary IMCs $(Cu, Ni)_6Sn_5$ and $(Ni, Cu)_3Sn_4$, based on the Cu_6Sn_5 and Ni_3Sn_4 crystal structure, were prevalent at the interface between the Ni-P layer and the Sn–Ag–Cu alloy during soldering and that Ag_3Sn precipitated in an elongated form in the Sn matrix of the Sn–Ag–Cu solder. Furthermore, Zeng [9,10] found that the IMC of $(Cu, Ni)_6Sn_5$ can grow significantly more quickly than Ni_3Sn_4. Habu et al. [11] and Kim et al. [3] pointed out that the addition of Ni and Ge improved anti-oxidation, tensile properties and lowered dross formation of solder. Moreover, the study had also been published that the addition of a small amount Ge in Sn–Ag–Cu solder alloy could improve the adhesion strength in BGA package [2].

The main purpose of this study is to investigate the formation of IMCs in Sn–Ag–Cu and Sn–Ag–Cu–Ni–Ge solder systems during soldering and subsequent long-term isothermal aging below the liquidus temperature. Also, small amounts of Ni and Ge were added to the Sn–Ag–Cu solder to investigate the microstructure of the interfacial IMCs between the Cu/Ni–P/Au metallized Ball Grid Array (BGA) substrate and the solder.

2. Experimental procedure

The types of lead-free solder balls investigated in this study were Sn–3.2Ag–0.5Cu and Sn–3.5Ag–0.5Cu–0.07Ni–0.01Ge (in wt.% and Sn balanced). Both types were 760 μm in diameter. The diameter of metallized BGA substrate was 600 μm. The thickness of the gold layer was less than 1 μm, while the nickel–phosphorus and copper layers were 5.4 and 30 μm thick, respectively.

* Corresponding author. Tel.: +886 6 2757575x62929; fax: +886 6 2759602.
E-mail address: pj.shih@msa.hinet.net (P.-C. Shih).

0925-8388/$ – see front matter © 2006 Elsevier B.V. All rights reserved.
doi:10.1016/j.jallcom.2006.11.036

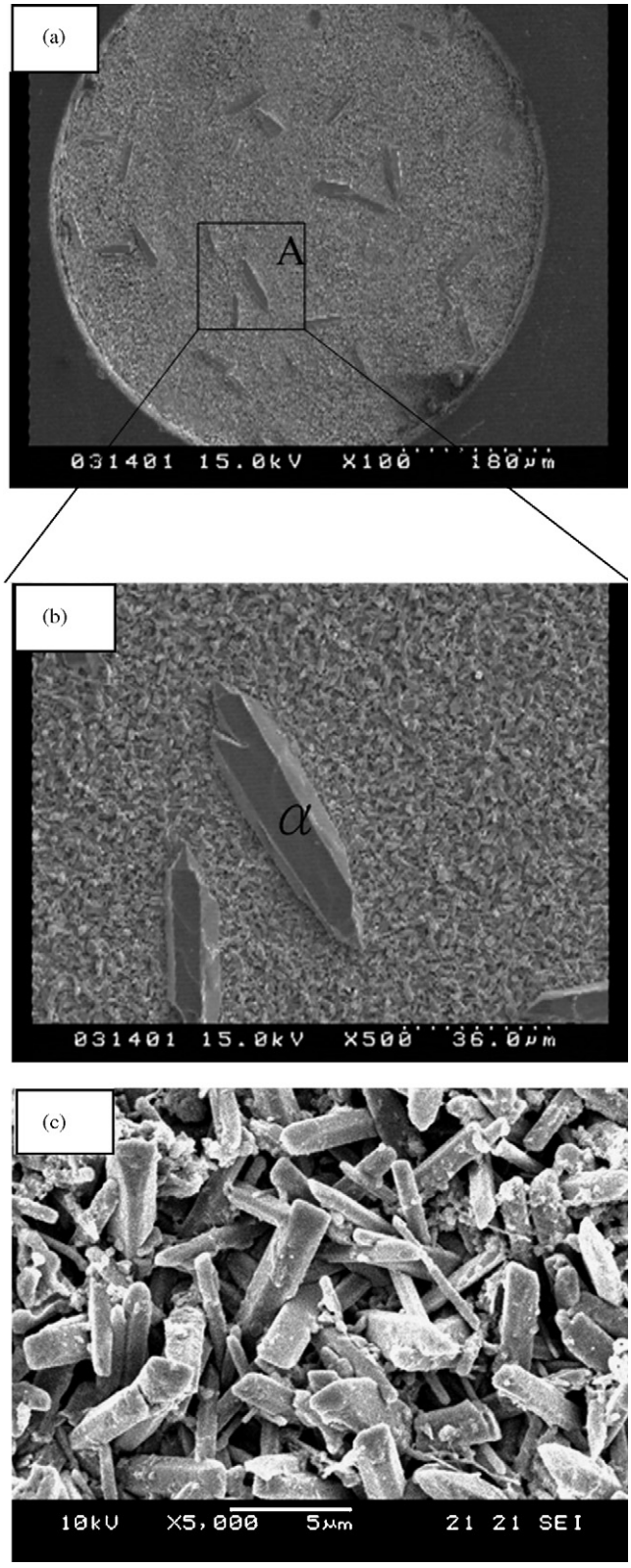

Fig. 1. The features of the interfacial IMCs formed between Sn–3.2Ag–0.5Cu solder and Cu/Ni–P/Au substrate in as-reflowed specimen (surface view, soldering temperature: 240 °C) (a) IMCs on the metallized pad (b) hexagonal IMC-α and (c) whisker-shaped IMC.

Before soldering, laboratory-prepared flux was smeared onto the substrate. A mold was used to apply the Sn–Ag–Cu or Sn–Ag–Cu–Ni–Ge solder balls, respectively, to each Cu/Ni–P/Au metallized solder pad on the substrate. The soldering process was performed in an IR (infrared) furnace under a protective atmosphere of 90%N_2–10%H_2. The reflow profile consists of an initial 30 s heating phase at 170 °C, which is then increased to a peak temperature of 240 °C for 30 s. After soldering, the package was subjected to thermal aging at 150 °C for 100–1000 h.

The cross section of the soldered samples was polished with 0.3 μm Al_2O_3 powder, and then etched with a 5% HCl–95%H_2O solution for interfacial investigation by scanning electron microscope (SEM), and energy dispersive X-ray analysis (EDX). The excess solder on the Cu/Ni–P/Au metallized substrates was removed with a 50%HNO_3–50% H_2O solution to reveal the surface of IMCs morphology.

3. Results and discussion

3.1. Surface morphology observations and interfacial formation behavior of IMC upon soldering

Fig. 1a shows the surface view of IMCs formed immediately after soldering between the Cu/Ni–P/Au metallized pad and the

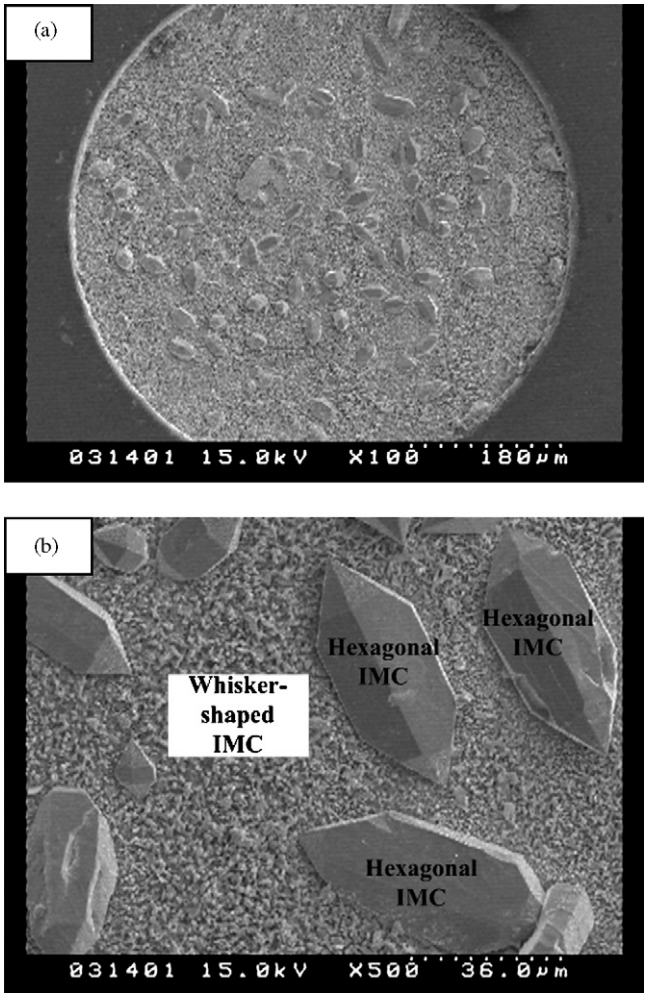

Fig. 2. The features of the interfacial IMCs formed between Sn–3.5Ag–0.5Cu–0.07Ni–0.01Ge solder and Cu/Ni–P/Au substrate in as-reflowed specimen (surface view, soldering temperature: 240 °C) (a) IMCs on the metallized pad and (b) hexagonal IMC and whisker-shaped IMC.

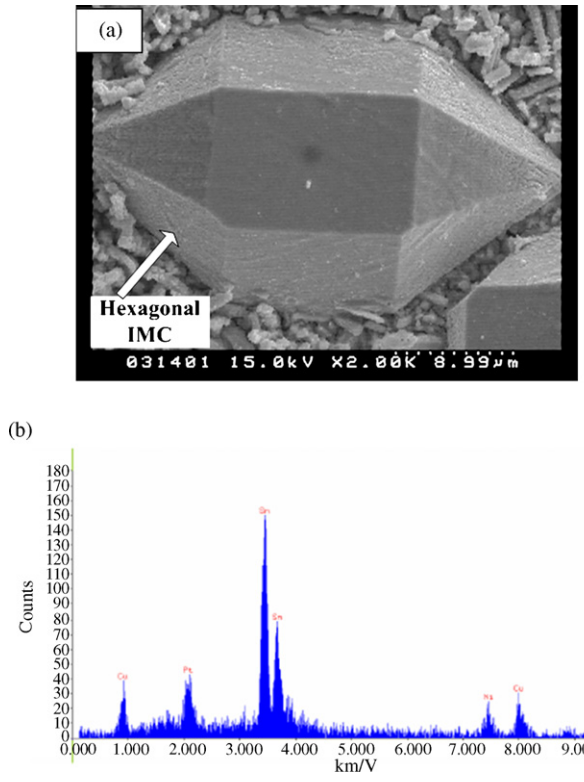

Fig. 3. The features of the hexagonal IMC in Sn–3.2Ag–0.5Cu solder system (a) surface view and (b) EDX analysis spectrum.

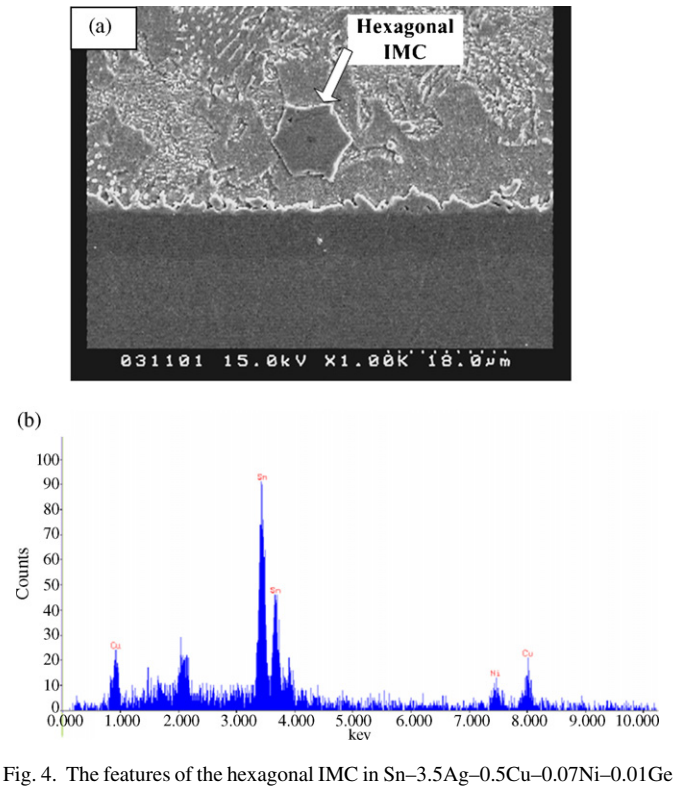

Fig. 4. The features of the hexagonal IMC in Sn–3.5Ag–0.5Cu–0.07Ni–0.01Ge solder system (a) cross section and (b) EDX analysis spectrum.

Sn–3.2Ag–0.5Cu solder. Fig. 1b, a magnification of region A in Fig. 1a, reveals that there are two different types of IMC located at the interface. One is an elongated hexagonal crystal intermetallic compound, labeled α, which is distributed randomly on the metallized pads. The other is the whisker-shaped crystal surrounding the hexagonal crystals. The dimensions of the former IMC are much larger than those of latter IMC, which are closed to 5 μm in length, as shown in Fig. 1c. Similar results are found in the Sn–3.5Ag–0.5Cu–0.07Ni–0.01Ge solder system as shown in Fig. 2a and b. The EDX analysis results show that the composition of the hexagonal IMCs in both solder systems are Cu:Ni:Sn = 39:19:42 (at.%) as shown in Fig. 3 and Cu:Ni:Sn = 36:20:44 (at.%) in Fig. 4. Hence, it seems that the Ge was not involved in Cu–Ni–Sn compounds. It could be ascribed to the small fraction of Ge in the Sn–3.5Ag–0.5Cu–0.07Ni–0.01Ge solder. Previous studies [12,13] indicated that Cu and Ni could substitute for each other in binary compounds with Sn. The EDX results and the ternary phase diagram of Sn–Cu–Ni [8] shown in Fig. 5 indicated that Ni atoms dissolve in Cu_6Sn_5 hexagonal crystal IMC reaching a maximum proportion of 25–27 at.% at 240 °C. Therefore, the hexagonal crystal IMC identified in this study could be $(Cu,Ni)_6Sn_5$ with Ni atoms dissolved in Cu_6Sn_5. The whisker-shaped intermetallic compounds without Ge content which surround the $(Cu,Ni)_6Sn_5$ compounds at the interface in both solder joints are, respectively, Ni:Cu:Sn = 37:10:53 and Ni:Cu:Sn = 36:9:55 (at.%). According to atomic stoichiometry, the whisker-shaped intermetallic compounds could be $(Ni, Cu)_3Sn_4$ with Cu atoms dissolved in Ni_3Sn_4 [8,12,13]. $(Ni, Cu)_3Sn_4$ with whisker-shaped morphology is possibly ascribed to anisotropic grain growth during interfacial reaction.

Figs. 6a, b and 7a show the cross section views of the $(Cu,Ni)_6Sn_5$ compounds, which are about 12 μm in thickness, and the $(Ni, Cu)_3Sn_4$ compounds. In addition to the IMCs mentioned previously, a plate-shaped intermetallic compound, 100 μm in length, is found within both solder systems as shown in Figs. 6c and 7b. The EDX results and the Ag–Sn binary

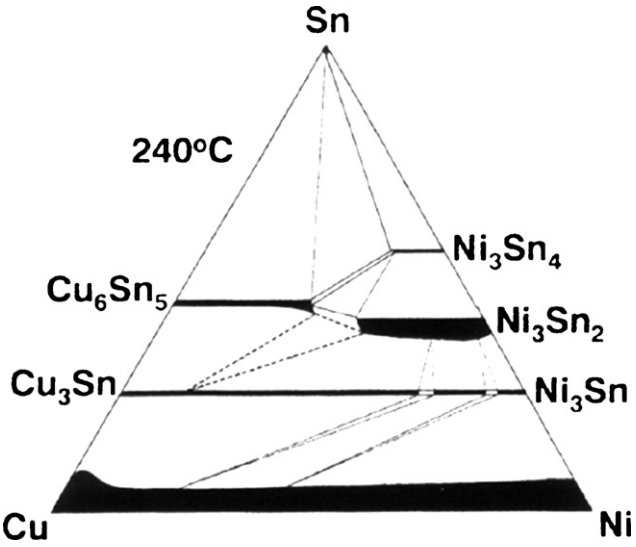

Fig. 5. The ternary phase diagram of Sn–Cu–Ni at 240 °C [8].

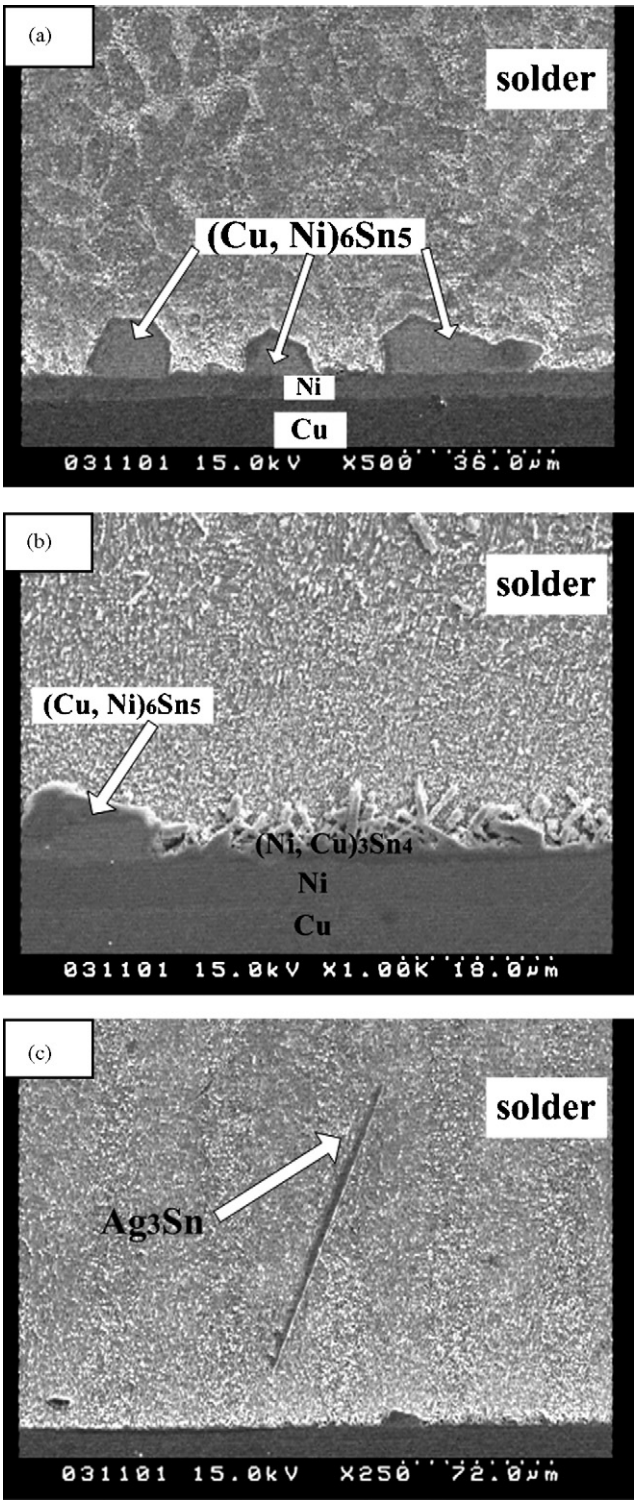

Fig. 6. The features of the interfacial IMCs formed between Sn–3.2Ag–0.5Cu solder and Cu/Ni–P/Au substrate in as-reflowed specimen (cross section, soldering temperature: 240 °C) (a) IMCs at the interface, (b) hexagonal $(Cu,Ni)_6Sn_5$ and whisker-shaped $(Ni,Cu)_3Sn_4$ and (c) plate-shaped Ag_3Sn.

phase diagram [14] indicated that the plate-shaped intemetallic compound is Ag:Sn = 72:28 (at.%) (possibly Ag_3Sn). A fourth particle-shaped IMC found in the solder region was also identified as Ag_3Sn, shown in Fig. 7. Au and Ge were not present

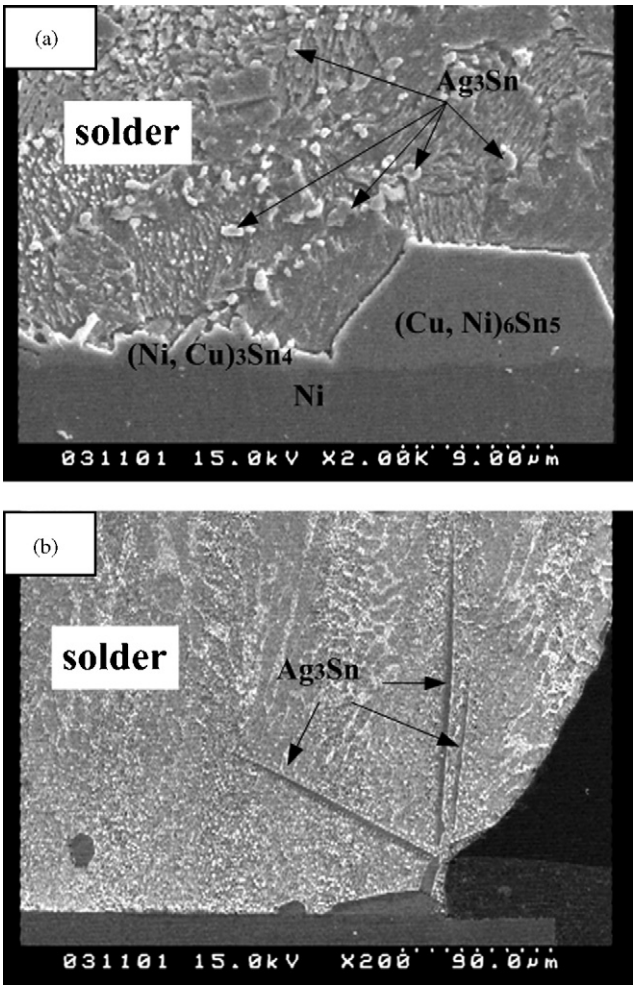

Fig. 7. The features of the interfacial IMCs formed between Sn–3.5Ag–0.5Cu–0.07Ni–0.01Ge solder and Cu/Ni–P/Au substrate in as-reflowed specimen (cross section, soldering temperature: 240 °C) (a) hexagonal $(Cu,Ni)_6Sn_5$ and whisker-shaped $(Ni,Cu)_3Sn_4$ and (b) plate-shaped Ag_3Sn.

in any of the compounds formed at the interface or within the solder. Also, the addition of the fractional Ge seems not to affect the microstructure of the interfacial IMCs noticeably. However, according to the previous study [2], Ge may dissolve in Sn to enhance the shear and tensile strengths of joints. The desirable Ge composition for Sn–Ag–Cu solder is unknown and the study on various Ge contents added to Sn–Ag–Cu solder joints is necessary to be carried out to realize the improved adhesion strength.

Fig. 8a shows that the plate-shaped Ag_3Sn contacts the $(Cu,Ni)_6Sn_5$ compounds. There is a notch close to 100 μm in length on the $(Cu,Ni)_6Sn_5$ compounds as shown in Fig. 8b (labeled B). This phenomenon may be attributed to the reaction of Sn with Cu and Ni to form the $(Cu,Ni)_6Sn_5$, while Ag atoms diffuse to react with Sn locally to form Ag_3Sn. Hence, these two types of IMCs are found quite close to each other. However, since a layer of Sn likely exists between the compounds, the etching solution washed away the fragile Ag_3Sn structure (Fig. 8b).

The distribution of $(Ni, Cu)_3Sn_4$ near $(Cu,Ni)_6Sn_5$ on the metallized pad for Sn–3.2Ag–0.5Cu and Sn–3.5Ag–

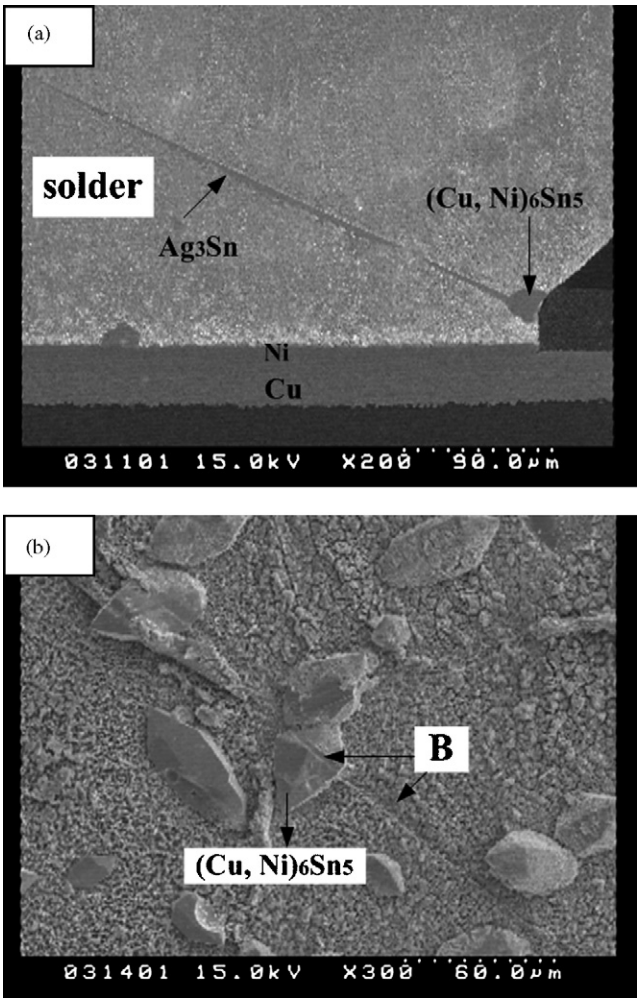

Fig. 8. The contact between hexagonal $(Cu,Ni)_6Sn_5$ and plate-shaped Ag_3Sn in (a) Sn–3.2Ag–0.5Cu (cross section) and (b) Sn–3.5Ag–0.5Cu–0.07Ni–0.01Ge (labeled B) solder systems.

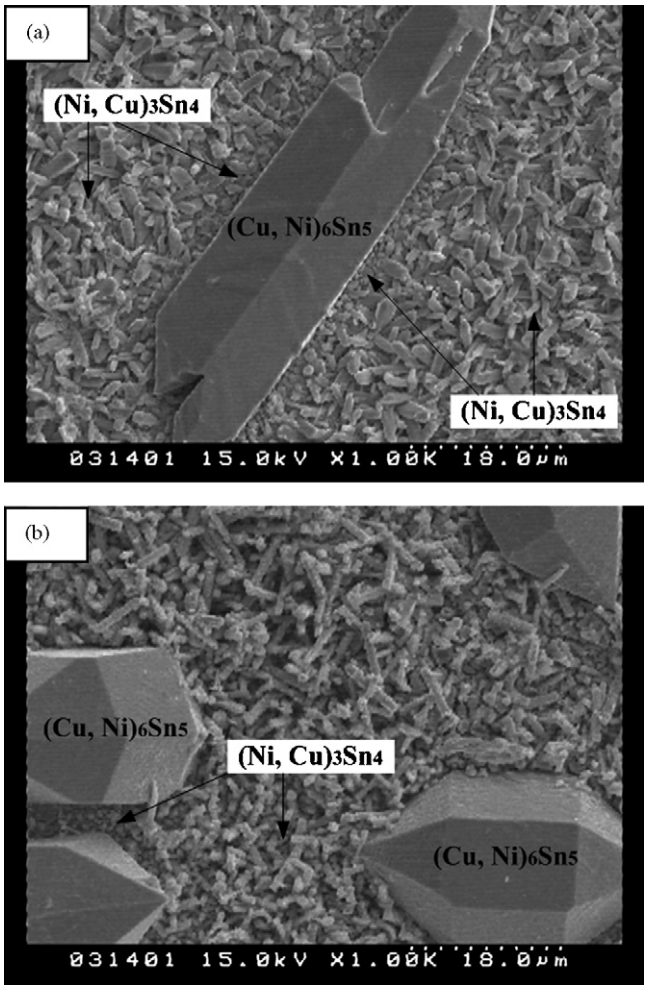

Fig. 9. The dimension differences between $(Ni,Cu)_3Sn_4$ crystals formed on the metallized pad near $(Cu,Ni)_6Sn_5$ (surface view) for (a) Sn–3.2Ag–0.5Cu solder system and (b) Sn–3.5Ag–0.5Cu–0.07Ni–0.01Ge solder system.

0.5Cu–0.07Ni–0.01Ge solder systems are, respectively, shown in Fig. 9a and b. The size of the $(Ni, Cu)_3Sn_4$ whiskers next to hexagonal $(Cu,Ni)_6Sn_5$ is significantly smaller than those of the whiskers that developed farther away. This indicates that Sn atoms are competed by Cu and Ni to form Cu–Sn and Ni–Sn compounds. It is possible that once Cu reacted with Sn to form the Cu–Sn compounds at the interface, nearby regions contain a low-concentration of Sn atoms. Smaller $(Ni, Cu)_3Sn_4$ whiskers form in these regions as a result.

As shown in Fig. 9a and b, the hexagonal $(Cu,Ni)_6Sn_5$ is composed of the same elements as the whisker-shaped $(Ni, Cu)_3Sn_4$ albeit in different proportions. It is of interest to see that these two types of compounds differ so much in dimension. The dissolved Cu (in Ni_3Sn_4 compounds) or Ni (in Cu_6Sn_5 compounds) may have effect on the crystal size. It was pointed out [15] that the transition metals play an important role in catalysis. Nickel is a typical transition metal while copper is a non-transition metal [16]. Ni atoms have a vacant 3d-orbital while Cu atoms do not. Therefore, the dissolved Ni atoms could catalyze the growth of $(Cu,Ni)_6Sn_5$ and lead to its increased size. However, the details of the behavior of Ni definitely need further study.

3.2. Surface morphology observations and interfacial formation behavior of IMC upon aging

Figs. 10 and 11 show the surface views of the $(Cu,Ni)_6Sn_5$ and $(Ni, Cu)_3Sn_4$ compounds formed at the interface after aging for 100–1000 h for Sn–3.2Ag–0.5Cu and Sn–3.5Ag–0.5Cu–0.07Ni–0.01Ge solder systems, respectively. The $(Ni, Cu)_3Sn_4$ compounds coarsen noticeably after heat treatment for 1000 h, while the $(Cu,Ni)_6Sn_5$ compounds do not. The Ge-rich phases are not observed even after 1000 h heat treatment. The lack of $(Cu,Ni)_6Sn_5$ grain growth could indicate that Cu atoms are restricted in the solder system (fixed at 0.5 wt.%) and that the Ni-P layer acts as a diffusion barrier that inhibits the movement of Cu atoms from the metallized pad. On the other hand, Ni atoms could be easily supplied from the Ni-P layer (5.4 μm). Hence, the $(Ni, Cu)_3Sn_4$ compounds are able to grow as the heat treatment process proceeds.

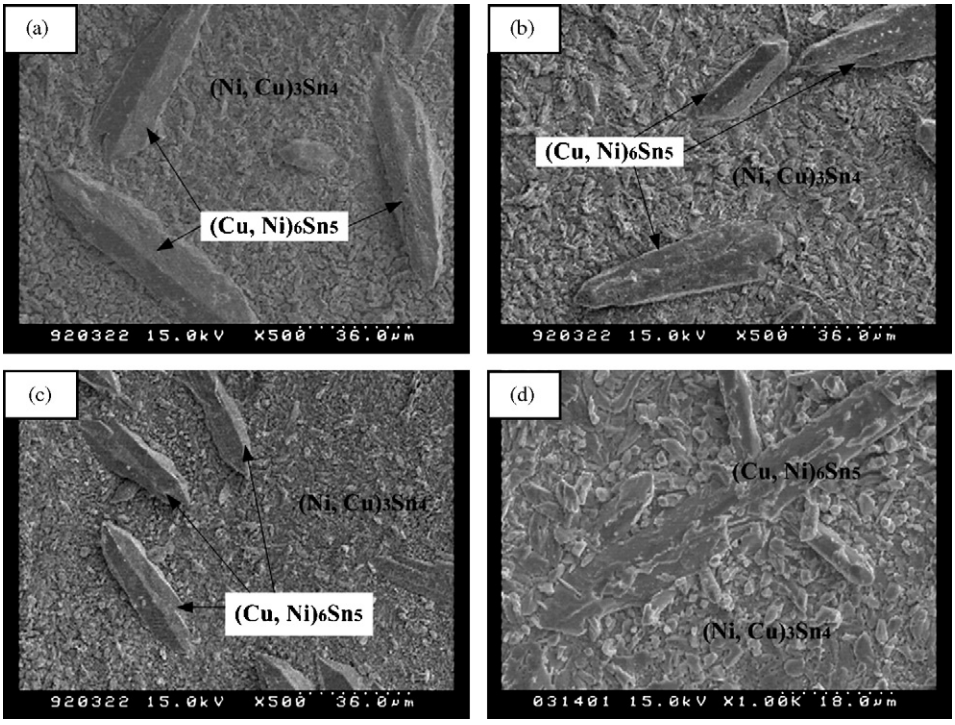

Fig. 10. The features of the interfacial IMCs formed between Sn–3.2Ag–0.5Cu solder and Cu/Ni–P/Au substrate during thermal aging test (surface view, soldering temperature: 240 °C) (a) 100 h (b) 200 h (c) 500 h and (d) 1000 h.

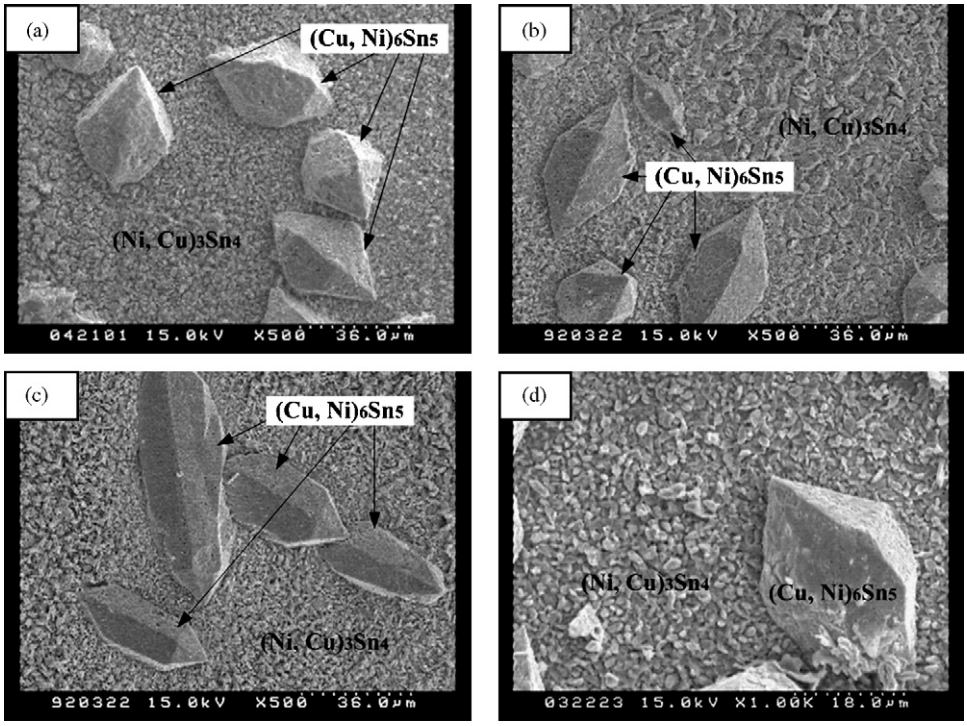

Fig. 11. The features of the interfacial IMCs formed between Sn–3.5Ag–0.5Cu–0.07Ni–0.01Ge solder and Cu/Ni–P/Au substrate during thermal aging test (surface view, soldering temperature: 240 °C) (a) 100 h (b) 200 h (c) 500 h and (d) 1000 h.

4. Conclusions

After soldering with either the Sn–3.2Ag–0.5Cu or the Sn–3.5Ag–0.5Cu–0.07Ni–0.01Ge solder system, the hexagonal $(Cu,Ni)_6Sn_5$ and the whisker-shaped $(Ni, Cu)_3Sn_4$ formed at the interface, while the small particle-shaped or plate-shaped Ag_3Sn compounds were observed within the solder itself. Au and Ge were not present in any of the compounds formed at the interface or within the solder after soldering. Moreover, the plate-shaped Ag_3Sn may exist in contact with the $(Cu,Ni)_6Sn_5$ compounds.

After heat-treating for 100–1000 h, the $(Ni, Cu)_3Sn_4$ compounds coarsened noticeably, while the $(Cu,Ni)_6Sn_5$ compounds did not. The addition of Ge seems not to significantly affect the microstructure of the interfacial IMCs. The Ag_3Sn compounds within the solder also coarsened near the interfacial IMC, and they did not directly contact the metallized BGA pads. The dissolved Ni atoms with a vacant 3d-ortital might catalyze the growth of $(Cu,Ni)_6Sn_5$ and lead to the different sizes of the $(Cu,Ni)_6Sn_5$ and the $(Ni, Cu)_3Sn_4$ compounds.

Acknowledgements

The financial support for this work, provided by the National Science Council of ROC (Taiwan) under grant NSC91-2216-E-006-035 is gratefully acknowledged. The authors also thank Accurus Inc. for supplying the solder balls.

References

[1] C.B. Lee, S.B. Jung, Y.E. Shin, C.C. Shur, Mater. Trans. 43 (8) (2002) 1858–1863.
[2] C.M. Chuang, P.C. Shih, K.L. Lin, J. Electron. Mater. 33 (1) (2004) 1–6.
[3] K.S. Kim, S.H. Huh, K. Suganuma, Microelectron. Reliab. 43 (2003) 259–267.
[4] C.M. Chuang, P.C. Shi, K.L. Lin, Proceedings of the Fourth International Symposium on Electronic Materials And Packaging, December 4–6, 2002, pp. 360–365.
[5] S.K. Kang, W.K. Choi, D.Y. Shih, P. Lauro, D.W. Henderson, T. Gosselin, D.N. Leonard, 52nd Proceedings on Electronic Components and Technology Conference, May 28–31, 2002, pp. 146–153.
[6] Y. Zheng, C. Hillman, P. McCluskey, 52nd Proceedings on Electronic Components and Technology Conference, May 28–31, 2002, pp. 1226–1231.
[7] Y.D. Jeon, S. Nieland, A. Ostmann, H. Reichl, K.W. Paik, 52nd Proceedings on Electronic Components and Technology Conference, May 28–31, 2002, pp. 740–746.
[8] C.E. Ho, R.Y. Tsai, Y.L. Lin, C.R. Kao, J. Electron. Mater. 31 (6) (2002) 584–590.
[9] K. Zeng, V. Vuornen, J.K. Kivilahti, 51st Proceedings on Electronic Components and Technology Conference, May 29th–June 1st, 2001, pp. 693–698.
[10] A. Zribi, L. Zavalij, P. Borgesen, A. Primavera, G. Westby, E.J. Cotts, 51st Proceedings on Electronic Components and Technology Conference, May 29th–June 1st, 2001, pp. 687–692.
[11] K. Habu, N. Takeda, H. Watanabe, H. Ooki, J. Abe, T. Saito, Y. Taniguchi, K. Takayama, Proceedings of EcoDesign '99: First International Symposium on Environmentally Conscious Design and Inverse Manufacturing, February 1–3, 1999, pp. 606–609.
[12] A. Zribi, A. Clark, L. Zavalij, P. Borgesen, E.J. Cotts, J. Electron. Mater. 30 (6) (2001) 1157–1164.
[13] T.B. Massalski, Binary Alloy Phase Diagrams, vol. 1, ASM, Metals Park, Ohio, USA, 1986, pp. 941–942.
[14] T.B. Massalski, Binary Alloy Phase Diagrams, vol. 1, ASM, Metals Park, Ohio, USA, 1986, p. 71.
[15] V.F. Kiselev, O.V. Krylov, Adsorption and Catalysis on Transition Metals and their Oxides, Springer-Verlag, 1989 (Chapter 2).
[16] T. Sasada, S. Ban, S. Norose, T. Nakano, Wear 159 (1992) 191–199.